

Simulating Prepreg Platelet Molding Compound Flexure Coupons in LS-DYNA[®] Using MAT54

Rebecca A. Cutting, Anthony J. Favaloro, Johnathan E. Goodsell

Composites Manufacturing and Simulation Center, Purdue University, West Lafayette, IN 47906

Abstract

Prepreg platelet molding compound (PPMC) is a composite material system primarily for compression molding comprised of rectangular platelets made from slit and chopped unidirectional prepreg. Prior to processing, the platelets are assumed to be in a planar random orientation state; however, this changes during molding as the platelet orientation state evolves in response to flow. The final orientations of the platelets affect the mechanical performance of manufactured components. As such, it is necessary to incorporate platelet orientations in simulations of PPMC parts to capture the material system behavior. This work introduces a modeling method for simplified PPMC geometries using MAT54 in LS-DYNA. A platelet generation code creates virtual PPMC samples with varying global orientation distributions. These orientations are input into LS-DYNA models of flexure coupons. A study is completed to understand how global platelet orientation affects the flexural stiffness and strength of the virtual samples. In addition, the results of the flexure simulations are compared to experimental results of flow-aligned PPMC coupons to validate the modeling method. The simulation study reveals that an increase in platelet alignment along the longitudinal axis of the sample results in an increase in flexural stiffness and strength in the models. This trend is confirmed experimentally, and the accuracy of the modeling method is discussed.

Introduction

In efforts to light-weight vehicles and increase fuel efficiency, automotive manufacturers have been investigating the use of carbon composites as alternatives to traditional materials on geometrically complex components of vehicles. Prepreg platelet molding compound (PPMC), a material system made from slit and chopped unidirectional prepreg, is one such promising option because it offers increased fiber volume fraction, and thus mechanical performance, compared to traditional composite molding compounds like sheet or bulk molding compounds. The stiffness and strength properties of PPMC are typically lower than that of the parent unidirectional (UD) tape (Kravchenko et al., 2018), but the increased processability and the ability of PPMC to form complex geometries makes it appealing for automotive applications.

PPMC can be provided in two forms: loose thermoplastic platelets or a sheet of thermoset platelets loosely bonded together during the manufacturing process. This work was completed with a sheet form of thermoset platelets (see Figure 1) made from a prepreg using Dow VORAFUSE M6400TM. The UD tape was processed in a machine that slit the prepreg along the fiber direction before chopping the slit sections along the transverse direction to form individual platelets with dimensions of 25.4 mm x 1.59 mm. The chopped platelets fell onto a moving conveyor belt and were subsequently heated slightly and compressed to form a mat. As the platelets did not fall onto the conveyor belt in a controlled fashion, the expected orientation state of the platelets within the sheet was in-plane uniform random.

The complexity of the meso-structure in this material system makes it difficult to model in commercial settings that are dependent upon simulation speed and model fidelity. If a simulated component of PPMC is to be eventually incorporated into a large assembly model, it is impractical to create a high fidelity model that captures every single platelet, as others have done in the past (Kravchenko et al., 2019).

This work introduces a modeling method for simplified PPMC geometries using shell elements and MAT 54 in LS-DYNA. PPMC flexure coupons with a specified global platelet orientation state are virtually created using a platelet generation code. The orientations are transferred into an existing baseline LS-DYNA model that simulates a flexure test according to ASTM D7264. The flexural stiffness and strength values are then calculated from the simulation results. A study is completed to understand how the mechanical properties are affected by the orientation state of the platelets within the sample. In addition, the simulation results are compared to experimental flexure results to determine the accuracy of the modeling method.



Figure 1: Prepreg platelet molding compound in sheet form

Setup of the Baseline Flexure Model

Before the effect of orientation state could be investigated on simulated flexure samples, it was prudent to create a functional baseline model. This allowed for the geometry, boundary conditions, and loading conditions to be simulated with a known unidirectional layup that could be compared to closed-form solution. Once the unidirectional model was verified, it was used as the basis for all PPMC flexure simulations. The model parameters were kept consistent across PPMC simulations, and the only variation between simulations was the orientation state defined. This ensured the resulting changes in stiffness and strength were solely a function of the orientation state of the platelets.

The unidirectional model followed standards for flexure testing associated with ASTM D7264. The test coupon was modeled to be 100 mm long and 13 mm wide. The bottom supports were set to a span of 76.8 mm and the top pin was positioned in the middle of these. In addition, the diameter of the support pins was 6.3 mm. All simulations and experiments performed in this work followed this dimensioned setup (see Figure 2) unless otherwise stated.

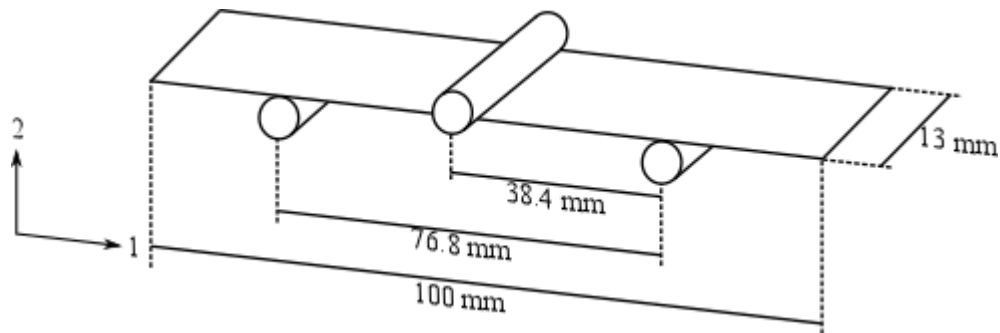


Figure 2: Dimensions of model and test

The flexure coupon was modeled with type-2 shell elements, and each element had in-plane dimensions of 0.7 mm x 0.7 mm. The bottom supports also used type-2 elements with dimensions of 1 mm x 1 mm and were defined as rigid. The top support was created using the *RIGIDWALL_GEOMETRIC_CYLINDER_MOTION_DISPLAY keyword. The cylinder was constrained to move vertically (in the 2-direction) at a rate of 0.4 m/sec for 0.025 sec. This resulted in a total displacement of 10 mm for the top pin. The simulated test speed was faster than the speed specified by ASTM D7264, but it was chosen after a convergence study on top pin speed showed it produced acceptable results. Figure 3 shows the mesh and setup for the baseline flexure model.

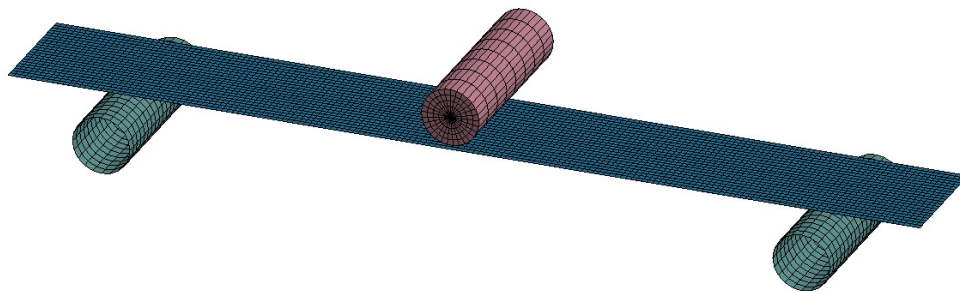


Figure 3: LS-DYNA model used for unidirectional simulations and PPMC simulations

Contact between components was defined using the *CONTACT_AUTOMATIC_SINGLE_SURFACE keyword with a segment-based contact type (SOFT=2). The dynamic (FD) and static (FS) coefficients of friction were set to 0.08, and the viscous damping coefficient (VDC) was set to 20%. Within the *CONTROL_CONTACT keyword, the scale factor for rigid wall penalties RWPNAL was set to -1.0 to prevent erroneous spikes in the recorded rigid wall reaction force data. Hourglass checks were initiated with the hourglass viscosity type (IHQ) set to 4 and the hourglass coefficient (QH) set to 0.1.

Two types of damping were applied to the virtual coupons: *DAMPING_GLOBAL with a damping constant (VALDMP) of 0.3 and *DAMPING_PART_STIFFNESS with a coefficient (COEF) set to 0.1.

The rigid wall reaction force (RWFORC) was the primary output of interest because it records the reaction force acting on the top pin. Therefore, within the *DATABASE_OPTION keyword, RWFORC was checked and set to output every 1e-08 sec. As the model contained orthotropic composites, the variable composite flag (CMPFLG) in the *DATABASE_EXTENT_BINARY keyword was set to 1 in order to ensure stress and strain data were output in the material coordinate system, and laminate shell theory (LAMSHT) was activated in *CONTROL_SHELL.

As previously stated, MAT 54, *MAT_ENHANCED_COMPOSITE_DAMAGE, was the material model selected for this work. The prepreg that served as the base for the platelet material system was used for the UD flexure coupons. The UD material properties were previously characterized and are reported in Table 1. The failure strains defined in MAT54 (DFAILT, DFAILC, and DFAILM) were all defined as the ultimate failure strains seen in experimental tension and compression tests.

Table 1: Material properties for unidirectional carbon fiber prepreg with VORAFUSE M6400

Material Property	Characterized Value	Test Standard
E1 [GPa]	114.0	ASTM D3039
E2 [GPa]	7.44	ASTM D3039
G12 [GPa]	5.73	ASTM D3518
XT [MPa]	1654	ASTM D3039
YT [MPa]	58.6	ASTM D3039
XC [MPa]	1113.5	Modified ASTM D695
YC [MPa]	234.6	Modified ASTM D695
S6 [MPa]	91.7	ASTM D3518

MAT54 has several parameters that are not measurable with a known ASTM standard (SLIMXX, SOFT). The values for these parameters were chosen based on trial and error and best practices by the authors. The complete MAT54 model used for this work is shown in Figure 4.

```
*MAT_ENHANCED_COMPOSITE_DAMAGE_TITLE
MAT054_FordDowMat
$#      mid      ro      ea      eb      (ec)      prba      (prca)      (prcb)
      1 1800.0000 1.00E+117.4400e+09 7.44E+09 0.017 0.017 0.017
$#      gab      gbc      gca      (kf)      aopt      2way
      5.73E+09 5.73E+09 5.73E+09 0.00 2.00 0.00
$#      xp      yp      zp      a1      a2      a3      mangle
      0.000 0.000 0.000 0.000 1.000 0.000 0.000
$#      v1      v2      v3      d1      d2      d3      dfailm      dfails
      0.000 0.000 0.000 1.000 0.000 0.000 0.035 0.230
$#      tfail      alph      soft      fbrt      ycfac      dfailt      dfailc      efs
      1E-09 0.000 0.500 0.000 2.000 0.014 -0.018 0.000
$#      xc      xt      yc      yt      sc      crit      beta
      1.11E+09 1.654E+09 2.35E+08 5.86E+07 9.17E+07 54.000 1.000
$#      pel      epsf      epsr      tsmd      soft2
      100.000 0.000 0.000 0.000 0.500
$#      slimt1      slimc1      slimt2      slimc2      slims      ncyred      softg
      0.200 0.800 0.200 0.800 1.000 0.000 1.000
```

Figure 4: MAT 54 property definitions for UD prepreg with VORAFUSE M6400

The layup of the UD samples was [0/90]_{4s}, and the orientation of each ply was defined as a single integration point through the thickness of the shell element. The number of integration points was set to 16 (the number of plies in the layup) using the *INTEGRATION_SHELL keyword. The thickness of the flexure coupon was defined as 2.0 mm.

Once complete, the simulation produced a rwrforc file, that contained load and time data points. The constant velocity of the top pin allowed for the production of the load-displacement curve. From there, the stress-strain curve was calculated using the geometry measurements of the simulated test coupon and the span of the lower supports (Carlsson et al., 2014). Figure 5 shows the stress-strain curve of the simulated UD coupon.

The raw data was noisy and showed significant oscillations due to the contact between the top pin and the sample, therefore, a moving average filter was applied to smooth out the results.

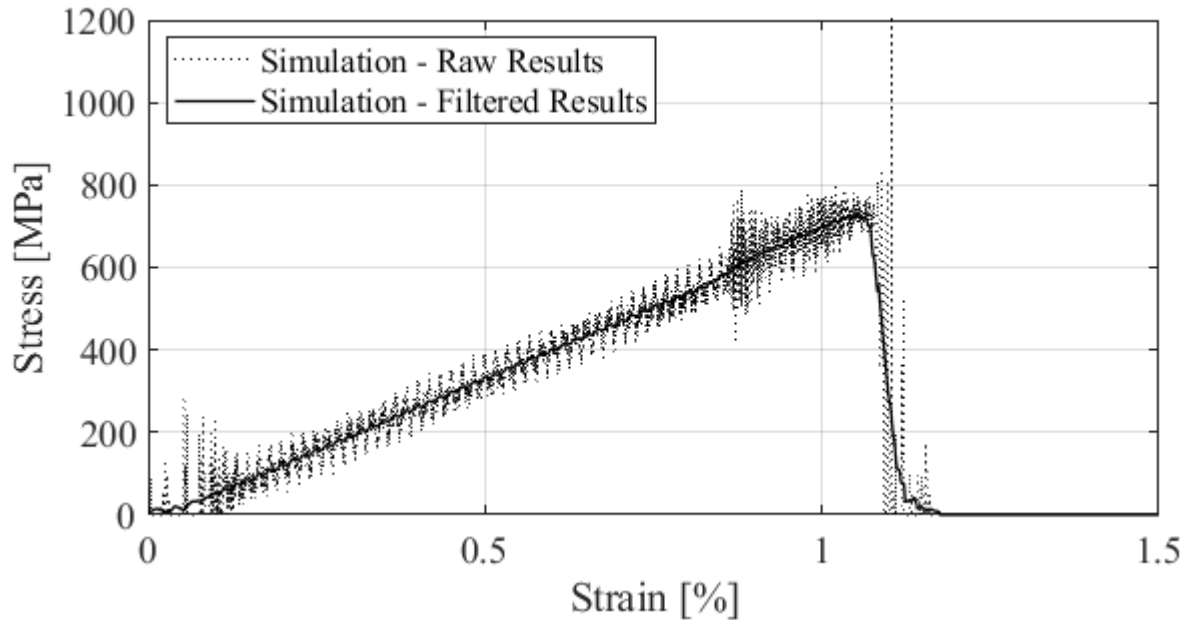


Figure 5: A moving average filter was applied to the raw results to smooth out the noisy and oscillatory behavior

In order to verify the UD model was functioning properly, it was necessary to compare the results to a trusted source in literature, like previous experimental studies or a closed-form solution. The mechanical response of a cross-ply laminate in flexure was documented by Pagano (Pagano, 1967) and Whitney (Whitney et al., 1974) in the mid-20th century. They stated it is possible to analyze cross-ply laminates using classical beam theory, but the modulus weighted moment of inertia must be used in the calculations. Once calculated, the weighted moment of inertia was incorporated into the standard equation for mid-span displacement of a beam in 3-point bending, and the stress-strain curve for the closed-form solution was derived from there. Figure 6 shows that the simulation of the cross-ply laminate in flexure matched well with the closed-form solution.

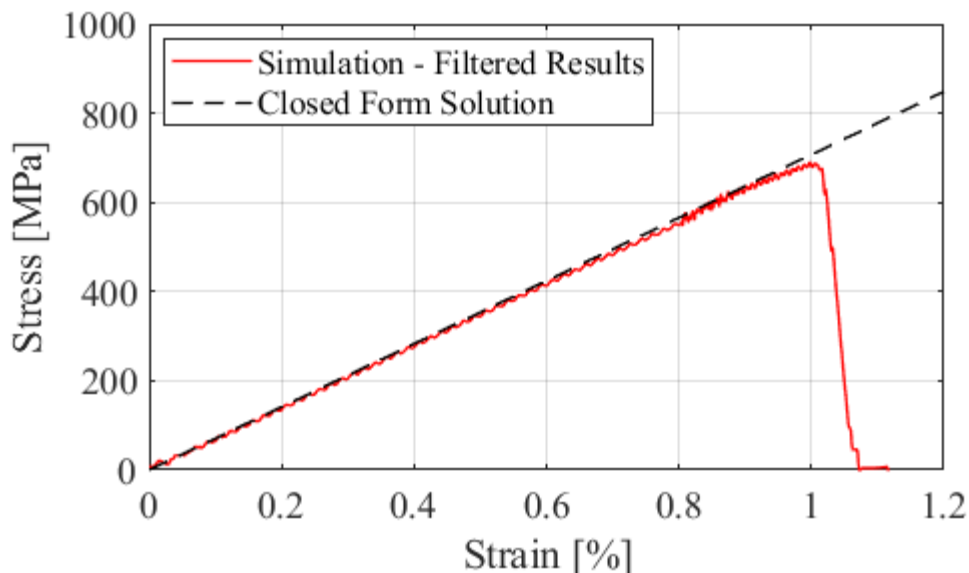


Figure 6: Comparison of the flexure simulation for a $[0/90]_4s$ laminate to the closed-form solution

Incorporating Platelet Orientations into the Baseline Model

Once the behavior of the baseline model was verified, orientation information was incorporated into the model to study the effect of platelet alignment on performance. Previous modeling work on PPMCs proved it was possible to capture flow behavior in PPMC molding (Favaloro et al., 2018) and the performance of test coupons (Kravchenko et al., 2019) using the properties of prepreg tape and assigning local fiber orientations to individual elements. This method was adopted for use with shell elements in LS-DYNA. The UD tape properties were input into MAT54 (as previously described), and each element within the model was then assigned an in-plane orientation angle to represent the platelet fiber direction. Groups of elements could have the same orientation definitions to represent a single platelet (see Figure 7).

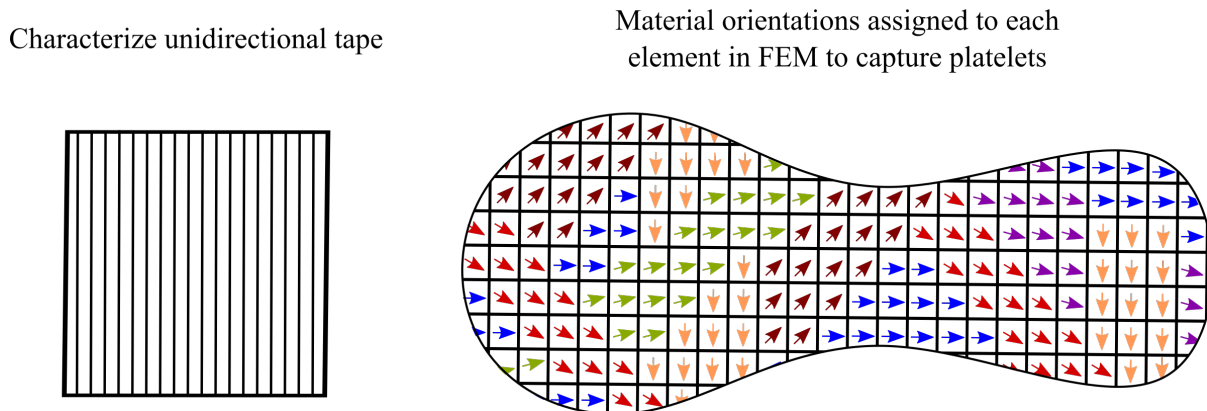


Figure 7: The modeling approached used characterized UD tape properties and assigned each element individual platelet fiber orientations

A platelet generation code created virtual flexure coupons with varying levels of platelet alignment (Cutting et al., 2017) that were then used to study the effect of platelet collimation on performance. The code allowed the user to request the number of platelet layers, the global level of collimation (A_{11} in the second-order orientation tensor), and the geometries of the coupon and platelets. The level of collimation, A_{11} , could vary from a value of 0 (representing no platelet collimation along the longitudinal axis of the sample) to 1 (representing complete platelet collimation along the longitudinal axis of the sample). Figure 8 shows four virtual coupons created with the platelet generation code with varying global A_{11} values. As the A_{11} value increases, there are more platelets aligned along the 1-direction.

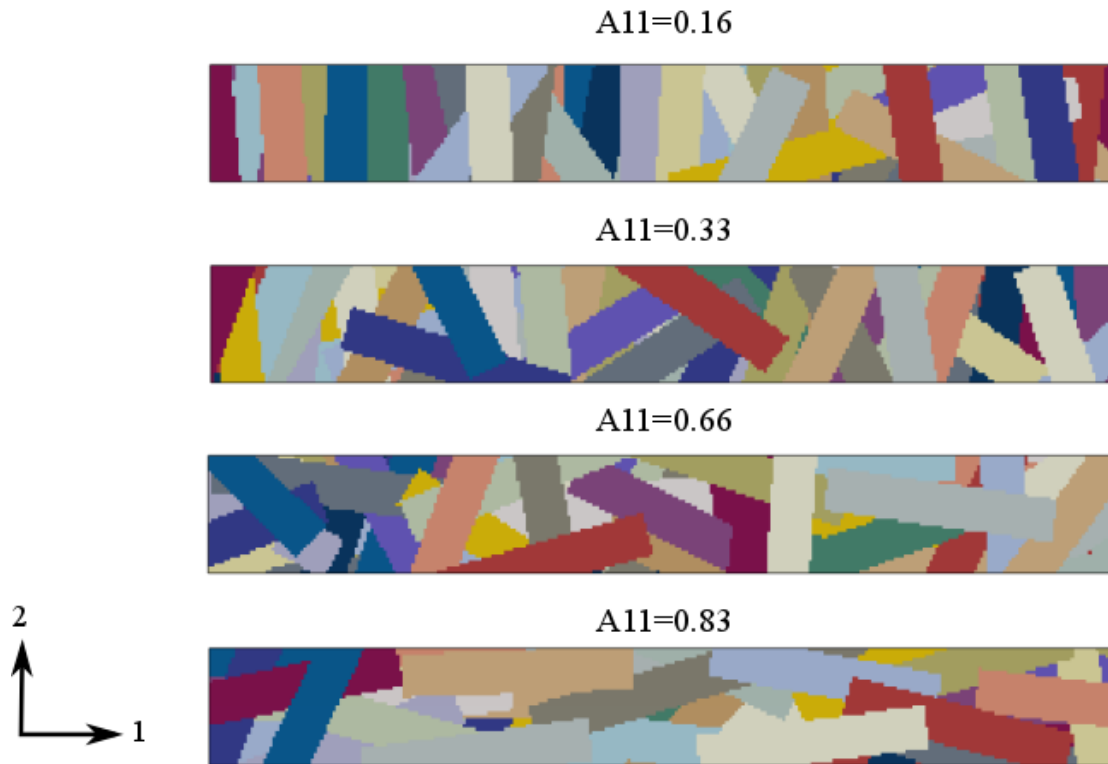


Figure 8: As the A11 value increases, the platelets begin to align and collimate along the 1-direction of the samples

The platelet generation code created 3-dimensional virtual coupons, and it was necessary to map the orientation information of each platelet over to the shell model within LS-DYNA. This was done by writing a Matlab script that converted vectors representing the fiber direction of the platelets to an in-plane orientation angle for a single integration point on a shell element (Figure 9 provides a visual example). The number of integration points (NIP) was determined by the number of platelets through the thickness. The ICOMP flag in *SECTION_SHELL was set to 1 to allow for in-plane fiber orientation angles, and the angles were applied to the BI variables. The PPMC coupons were given a 2.7 mm thickness and had 30 platelet orientations defined for each shell element. A total of 40 virtual coupons were created and ran with A11 values varying from 0.16 nominally to 0.83.

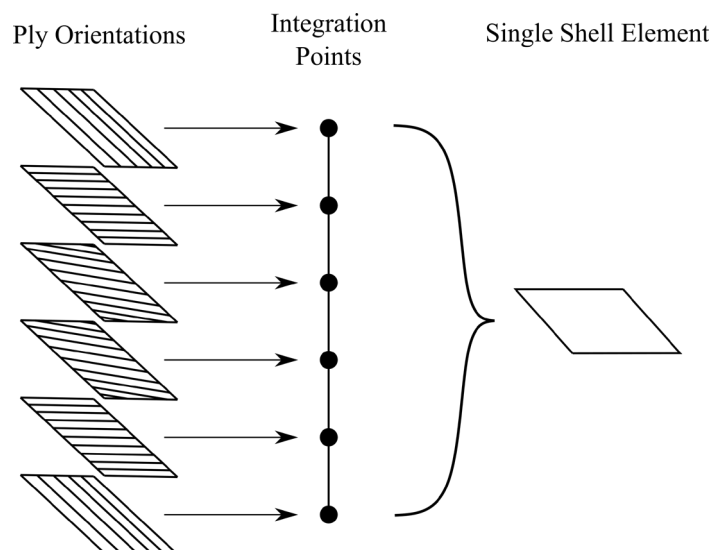


Figure 9: A fiber orientation angle is created for each platelet and applied to a single integration point in the shell element

Results and Discussion

The stress-strain curve, flexural modulus, and strength were recorded for each virtual coupon. Figure 10 shows the stress-strain curves for the 40 models. As the collimation of platelets increased along the longitudinal axis, the virtual coupon increased in stiffness and in strength. There are two noticeable outliers, one model with $A_{11} = 0.33$ and one model with $A_{11} = 0.83$. These likely failed prematurely due to a local transverse alignment near the loading surface.

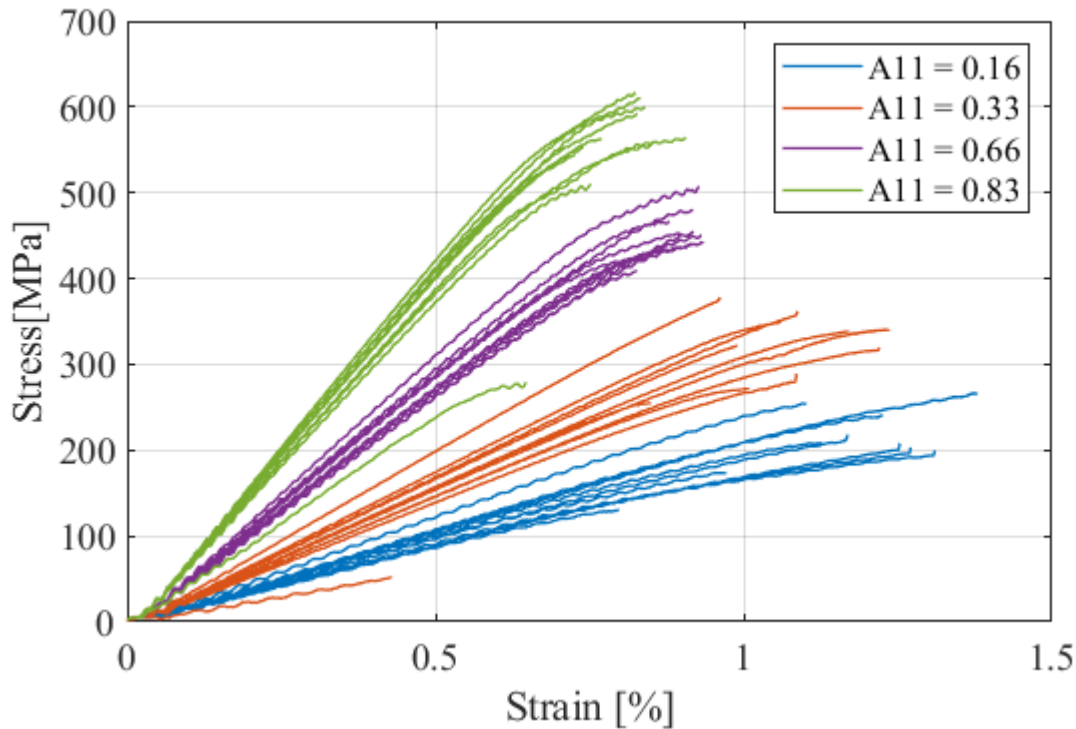


Figure 10: Stress-strain curves for 40 models with varying levels of platelet collimation

About 80 PPMC flexure coupons coming from 6 different plates were tested to compare to the simulation results. Each of the plates were manufactured with one of four different sized initial charges to obtain a range of flow alignment within the final plate. Common methods of estimating A_{11} include CT scanning parts (Denos et al., 2018) and using microscopy images (Sharp et al., 2019). Unfortunately, one of these methods is not cost effective, and the other is not yet suited for analyzing a large number of samples. For the purpose of this article, laminate theory techniques were adapted to perform orientation averaging on PPMC coupons to estimate the A_{11} value based on the experimental flexural modulus. This method reduced the number of input material properties required to estimate mechanical properties of the PPMC coupons. The UD material properties were input in the model to obtain the orientation averaged stiffness of samples with varying platelet alignments. The A_{11} was then back-calculated from the experimental flexural modulus.

Figure 11 plots the expected stiffness versus A_{11} curve from the orientation averaging technique, the experimental stiffness versus estimated A_{11} , and the simulated stiffness versus known A_{11} Samples were cut along the flow direction (longitudinal) and transverse direction in each plate, and are colored blue and red in the plot respectively. As can be seen, the simulated stiffness lines up well with the expected stiffness curve from the orientation averaging technique, showing that this PPMC modeling method captures global stiffness changes due to platelet orientation variation.

In addition, the plates with the smallest initial charge widths produced the highest and lowest stiffnesses confirming that increased flow corresponded to increased alignment of the platelets. The A11 estimation method forced the experimental results to lie perfectly on the orientation averaging curve, which is likely not the case in reality, but it provides a first estimate of the orientation state based on laminate theory.

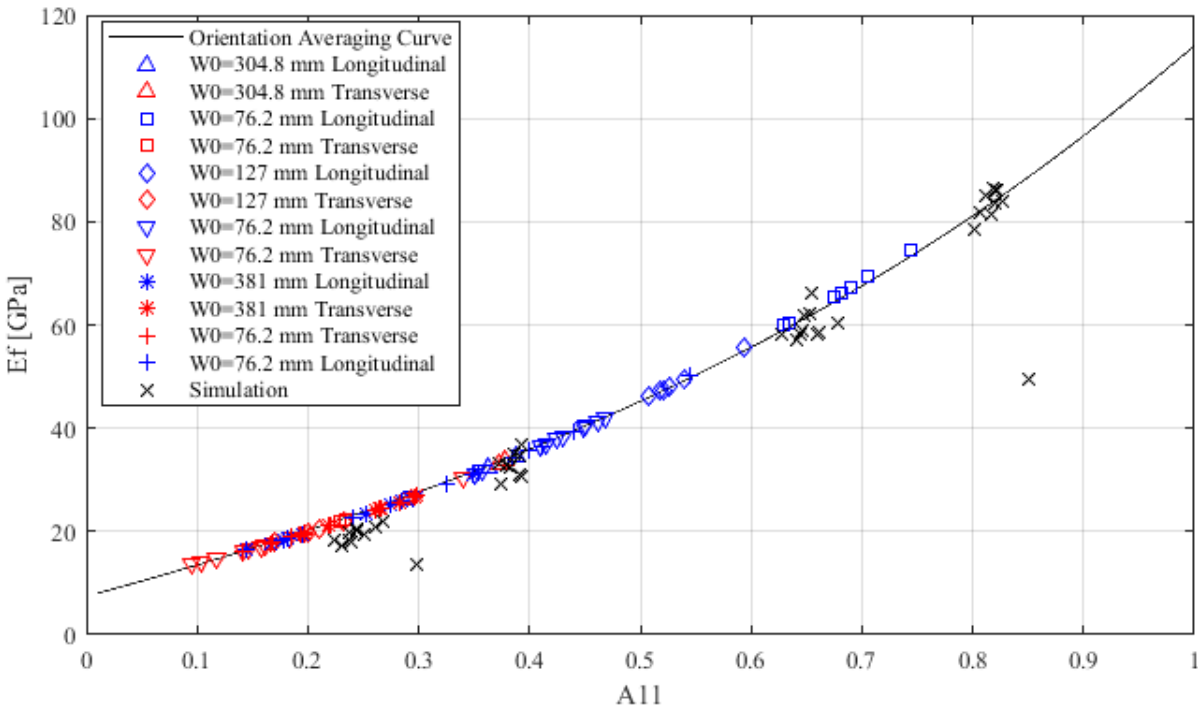


Figure 11: Orientation averaged stiffness and simulated stiffness versus A11

The experimental and simulated strengths versus A11 were then compared (see Figure 12) to the estimated and known A11 values respectively. The simulated strength from A11 was consistently lower than the experimental results with the largest margin of difference coming at the highest A11 values. There were a few potential causes of this discrepancy, one being the failure criteria associated with MAT54 and the other being UD material properties being too stiff in simulations to properly represent PPMC components. The transverse aligned coupons showed the lowest strength values while the longitudinal samples had the highest strength values. This again confirms that the amount of flow during the manufacturing process affects the alignment of the platelets and thus the mechanical performance.

This work introduced a novel way of modeling PPMC in LS-DYNA using shell elements and MAT54. First a baseline model was constructed and verified for a cross-ply laminate. Once functional, orientation information from virtual PPMC samples was applied to the baseline model to study the effect of global platelet orientation state on stiffness and strength. It was found that applying platelet orientation angles to integration points within shell elements provides enough mesostructure information to capture the variations of stiffness as a function of global platelet orientation state. A correlation was also found between strength and platelet collimation, but the simulation strengths were consistently below experimental results. There are built-in limitations with this simulation method, in that out-of-plane platelets cannot be modeled. In addition, delamination cannot be captured by modeling a single layer of shell elements. Next steps include improving the strength prediction and determining the level of platelet orientation fidelity necessary to capture the stiffness trends.

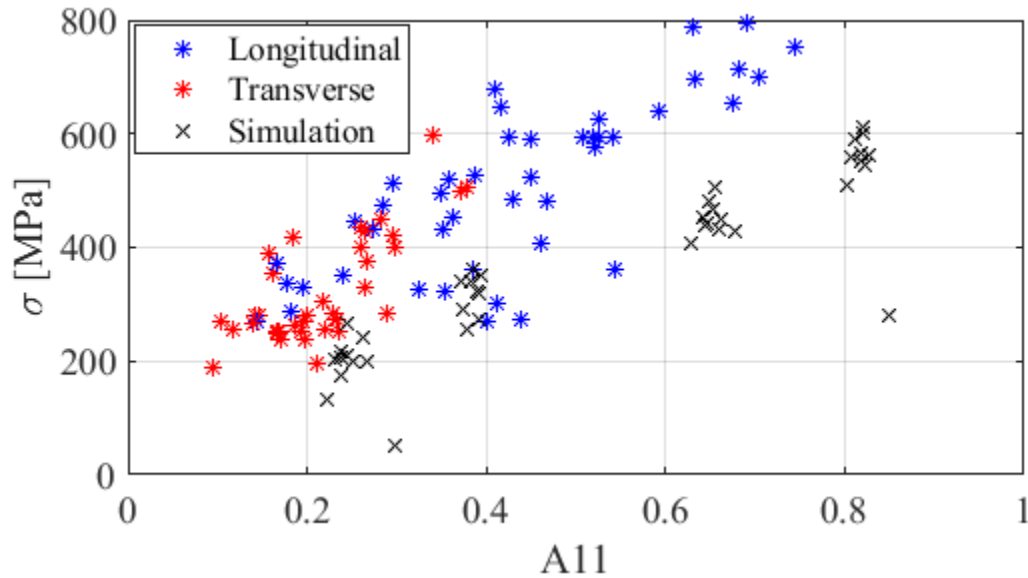


Figure 12: Experimental and simulated strengths versus estimated and known A11 values respectively

References

- Carlsson, L. A., Adams, D. F., & Pipes, R. B. (2014). *Experimental Characterization of Advanced Composite Materials* (4th ed.). CRC Press.
- Cutting, R. A., Favaloro, A. J., Goodsell, J. E., & Pipes, R. B. (2017). Determining Elastic Properties from the Dynamic Response of Discontinuous Fiber Composites. *American Society for Composites*.
- Denos, B. R., Sommer, D. E., Favaloro, A. J., Pipes, R. B., & Avery, W. B. (2018). Fiber orientation measurement from mesoscale CT scans of prepreg platelet molded composites. *Composites Part A: Applied Science and Manufacturing*, 114, 241–249. <https://doi.org/10.1016/J.COMPOSITESA.2018.08.024>
- Favaloro, A. J., Sommer, D. E., Denos, B. R., & Pipes, R. B. (2018). Simulation of prepreg platelet compression molding: Method and orientation validation. *Journal of Rheology*, 62(6), 1443–1455. <https://doi.org/10.1122/1.5044533>
- Kravchenko, S. G., Sommer, D. E., Denos, B. R., Avery, W. B., & Pipes, R. B. (2019). Structure-Property Relationship for a Prepreg Platelet Molded Composite with Engineered Meso-Morphology. *Composite Structures*, 210, 430–445. <https://doi.org/10.1016/j.compstruct.2018.11.058>
- Kravchenko, S. G., Sommer, D. E., & Pipes, R. B. (2018). Uniaxial strength of a composite array of overlaid and aligned prepreg platelets. *Composites Part A: Applied Science and Manufacturing*, 109, 31–47. <https://doi.org/10.1016/J.COMPOSITESA.2018.02.032>
- Pagano, N. J. (1967). Analysis of The Flexure Test of Bidirectional Composites. *Journal of Composite Materials*, 1, 336–342. <https://journals.sagepub.com/doi/pdf/10.1177/002199836700100402>
- Sharp, N., Goodsell, J., Favaloro, A., Sharp, N. D., Goodsell, J. E., & Favaloro, A. J. (2019). Measuring Fiber Orientation of Elliptical Fibers from Optical Microscopy. *Journal of Composites Science*, 3(1), 23. <https://doi.org/10.3390/jcs3010023>
- Whitney, J. M., Browning, C. E., & Mair, A. (1974). Analysis of the Flexure Test for Laminated Composite Materials. *Composite Materials: Testing and Design*, 30–45. <https://compass.astm.org/download/STP35481S.3118.pdf>